Time-Dependent Ginzburg-Landau Equation - Traveling Front

Or Hostezky

June 2022

1 Introduction

The Time-Dependent Ginzburg-Landau Equation (**TDGLE**) is a type of reaction-diffusion equation. The name reaction-diffusion derives from the fact that it introduces into the time-derivative of the solution the spatial effects of diffusion and a characteristic reaction function, which depends on the values of the solution themselves, on a local level. As its name implies, it can describe (as a generic example) the density of particles going through chemical reactions and are subjected to diffusion, when considering the continuum limit. In its most general form, the TDGLE in one dimension is given by

$$\frac{\partial u}{\partial t} = D\frac{\partial^2 u}{\partial x^2} + f(u) \quad , \tag{1}$$

where u can be regarded as a particle density, D is the diffusion coefficient and $f(u)$ is the reaction function, which describes the chemical nature of the system.

Specifically, the TDGLE involves a bistable reaction function, which by itself has two stable fixed points, introducing two stable phases to which the solution tends to at long times, depending on the initial condition, and at which the solution can stay indefinitely, given no gradients that generate active diffusion. Subsequently, if solved on an infinite spatial interval, a non-stable phase exists in between these two stable phases, in which the solution is not attracted to each of them.

In this work, a generic cubic reaction function is considered, namely $f(u) = -k(u-u_1)(u-u_2)(u-u_3)$ for $k > 0$ and $u_1 < u_2 < u_3$. Keeping the solution between u_1 and u_3, we take u_1 to be zero without the loss of generality. The resultant $f(u)$ (see Fig. 1 for a rescaled version) describes several types of chemical reactions. Namely, particles can split (being created at a rate proportional to their density u) or fuse together (hence negative terms proportional to u^2 and u^3, which are related to the probabilities for two or three particles to collide, respectively).

Rescaling the problem, we can measure time in units of k^{-1}, distance in units of $\sqrt{\frac{D}{k}}$ and the solution u and the parameter u_3 in units of u_2. Then, taking $u_2 = 1$, again without changing the dynamical nature of the equation, we arrive at the form

$$\frac{\partial u}{\partial t} = \frac{\partial^2 u}{\partial x^2} - u(u-1)(u-u_3) \quad . \tag{2}$$

Due to the fact that there are two stable phases in the infinite problem, a competition between the two can be generated by feeding the equation with an initial condition $u_0(x)$ that fulfills boundary conditions $u_0(x \to -\infty) = u_3$ and $u_0(x \to -\infty) = u_1$, with a region of (not too bizarre) transition between the phases, that will create an invasive wavefront situation, where one of the phases eventually takes over the other and dominates all space at $t \to \infty$. Therefore, for such initial conditions, it is expected that the dynamics will converge towards a traveling front solution, i.e. that $u(x,t) = u(x-ct)$, where the magnitude and sign of its velocity c are determined by the shape of the reaction function $f(u)$, as shall be explained below. Note that any large enough interval $[a,b]$ will produce such dynamics, given that the initial condition consists of a relatively localized transition region, much smaller than the size of the system, and that it fulfills the boundary conditions at this interval, that is, $u_0(x \to a) \to u_3$ and $u_0(x \to b) \to u_1$.

Defining the traveling coordinate, $\xi \equiv x - ct$, and plugging $u(\xi)$ into Eq. 2, we get an ODE instead of a the aforementioned PDE, namely,

$$\frac{d^2 u}{d\xi^2} + \frac{du}{d\xi} - u(u-1)(u-u_3) = 0 \quad . \tag{3}$$

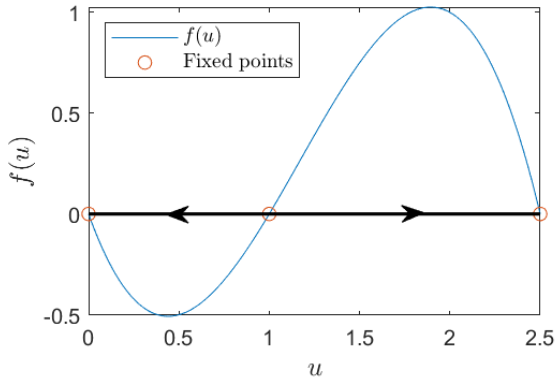

Figure 1: *Reaction function.* The chosen rescaled reaction function for analysis, $f(u) = -u(u-1)(u-u_3)$, as a function of the dynamic variable u (e.g. particle density), for $u_3 = 2.5$. Zero crossings of $f(u)$ (i.e. fixed points of u) are encircled in the graph. Streamlines of dynamics are shown to emphasize the bistable nature of this reaction function. The ratio between the areas under the curve at $0 < u < 1$ and $1 < u < u_3$ is detrimental to the dynamics of the traveling front solution (see *"area rule"* in the text below).

Under these conditions, this ODE can be solved analytically by assuming a monotonically decreasing solution in space at long times, with a derivative with a parabolic profile in u, namely

$$\frac{\partial u}{\partial x} = \frac{du}{d\xi} = Au(u-u_3)\ , \quad A > 0 \quad . \tag{4}$$

Note that this expression is indeed non-positive for $0 \leq u \leq u_3$. After integrating this equation and doing some basic algebra, we get a traveling front solution with an asymptotic form

$$u(\xi) = \frac{u_3}{1+\exp\left(\frac{u_3}{\sqrt{2}}(\xi-\xi_0)\right)} \quad , \tag{5}$$

such that the $u(\xi_0) = \frac{u_3}{2}$ for some ξ_0 that is determined by the initial condition and u_3. Moreover, substituting the ansatz in Eq. 4 into the derivatives in Eq. 3 gives an expression for the velocity of the traveling front, namely

$$c(u_3) = \frac{1}{\sqrt{2}}(u_3 - 2) \quad . \tag{6}$$

Note that this result is in agreement with the *"area rule"* or *"Maxwell's rule"*, which states that $c \sim \int_0^{u_3} f(u)du$, i.e. the globally stable phase (which will eventually dominate over the other) is determined by the larger area of the two areas under the curve of $f(u)$, at the intervals $0 < u < 1$ and $1 < u < u_3$ (Fig. 1). This result can be derived by plugging the traveling front ansatz directly to Eq. 1, multiplying by $\frac{du}{d\xi}$, integrating and using the boundary conditions for the traveling front solution, therefore it is valid for a generic bistable $f(u)$. For the chosen polynomial, the two areas are equal when $u_3 = 2$, which is exactly where $c = 0$ according to Eq. 6, and no phase takes over (due to no "traveling" of the front whatsoever). Thus, it is expected that for larger values of u_3, the traveling front will have a positive velocity, such that the u_3 phase will take over as $t \to \infty$, and vice versa.

2 Results

The chosen rescaled TDGLE (Eq. 2) was numerically solved by *MATLAB*'s built-in PDE solver *pdepe*, which discretizes space and integrates the ODEs resulting from this spatial discretization to obtain the approximate solutions at the desired times.

In order to approximate the dynamics of the problem on an infinite spatial interval, the boundaries were chosen such that the structure of the traveling frontfront is always far from each of them, according to the theoretically expected velocities. This is plausible since for convenience we use only symmetric

initial conditions, which give values of ξ_0 that are of order $\mathcal{O}(1)$, such that the wavefront at time t is located around $x \sim ct$. Namely, the rescaled TDGLE was solved on a finite interval $[a, b]$ where $a < 0 < b$, such that $|c|t_{final} \ll |a|, |b|$, t_{final} being the last point in time at which the solution is evaluated. Since both left and right propagating traveling fronts, and velocities that are no larger than 1 in magnitude are considered in this work, we take $|a| = |b| = 100$ for simplicity, which proves to be sufficient in the rescaled case. It is also made sure that each of the initial conditions used (see top panel of Fig. 3) is sufficiently close to, or is identically zero, at the boundaries. Accordingly, the boundary conditions used are consistent with the monotonically decreasing traveling front solution and initial conditions, namely $u(x = a, t) \approx u_3$ and $u(x = b, t) \approx 0$.

Due to the lack of sufficient theory (that I am aware of) regarding the times needed for the solution to converge into a traveling front with a shape as in Eq. 5 and velocity as in Eq. 6, the solution of the TDGLE was first tested at a range of different u_3 (c) values and with different initial conditions, in order to gain some basic intuition regarding both these aspects of convergence. At each case, the location of the wavefront through time was tracked, using the value of x where the solution is midway between the two stable phases, i.e. a time series $x_{front}(t)$ was obtained such that $u\big(x_{front}(t), t\big) = \frac{u_3}{2}$. The solution is then compared with the corresponding linear fit (starting at $t = 2$), which serves as its

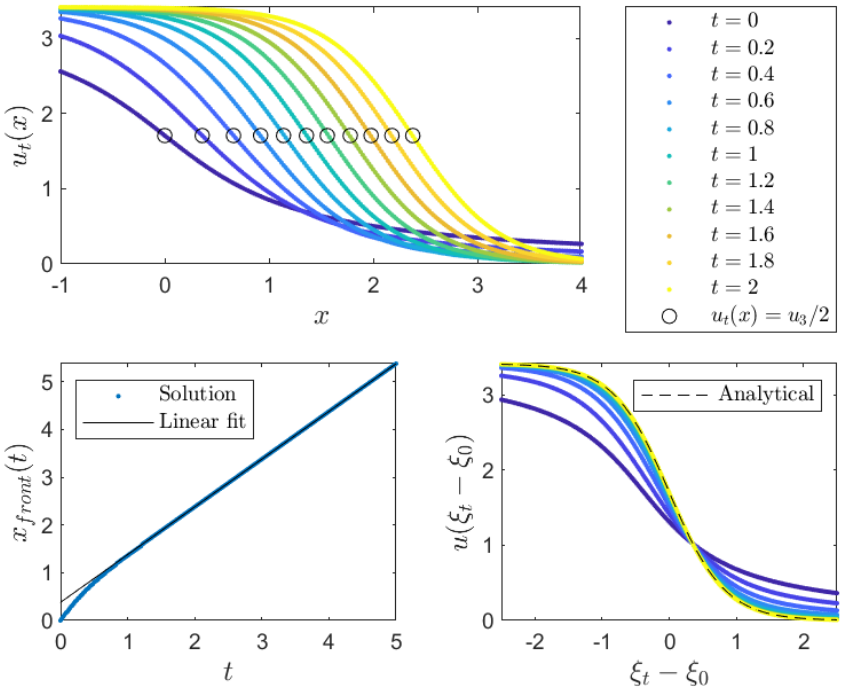

Figure 2: *Dynamics of the TDGLE, computing the velocity c of the traveling front.* **Top,** the solution of the TDGLE at several, equally spaced points in time (see legend), with an initial condition $u_0(x) = \frac{u_3}{\pi}\left(\frac{\pi}{2} - \tan^{-1}(x)\right)$, for the case of $u_3 = 2 + \sqrt{2}$, solved in the interval $x \in [-100, 100]$. Points where the solution is at half way between the two stable phases $u = 0$ and $u = u_3$, which were used in order to track the front of the traveling front at all times, are marked in circles. **Bottom left,** x values of the solution front, namely points x_{front} such that $u(x_{front}, t) = \frac{u_3}{2}$, are shown as a function of time in blue. A linear fit is imposed on the data in black, showing a convergence to a constant slope, which is the velocity c of the traveling front that emerges after convergence. **Bottom right,** convergence of the shape of the traveling front to the long-time solution in Eq. 5. The solution is shown at the same time-points as in the top panel, as a function of the space-time coordinate $\xi = x - ct$, c being the slope $x_{front}(t)$. The coordinate ξ is shifted by such ξ_0 that gives $u(\xi = \xi_0) = \frac{u_3}{2}$ after convergence. It is chosen by the initial condition, and is given by the constant coefficient from the linear fit to $x_{front}(t)$. The analytical shape of the traveling front at long times (Eq. 5) is imposed as a dashed line for comparison.

asymptotic limit (meaning that there is no "overshoot" such that the solution crosses the fit, whether the first starts below or above the latter), in order to check for convergence. Since we are interested in characterizing the dynamics after convergence, it must be made sure that the wavefront travels at a constant velocity, as expected from the analytical prediction. Such linear fit provides us with the values for the wavefront velocity c and initial shift ξ_0 between fit and spatial origin, which in our case is right where the front is at $t = 0$ (see bottom-left panel of Fig. 2), due to the spatial symmetry of our initial condition around this point.

Since convergence is monotonic in nature, such that the solution and corresponding linear fit are the closest at $t \sim t_{final}$ (since again, the fit is an *asymptote*), it is sufficient to ensure that $x_{front} - ct - \xi_0$ is close to its convergence values, which gives the time when the slope of x_{front} tends to c. Conveniently, the shape of the solution converges to the theoretical result in Eq. 5 at times comparable to those at which $c(t) \approx c(t \to \infty)$. For a visualization and a detailed account of the analysis process at a generic case, see Fig. 2.

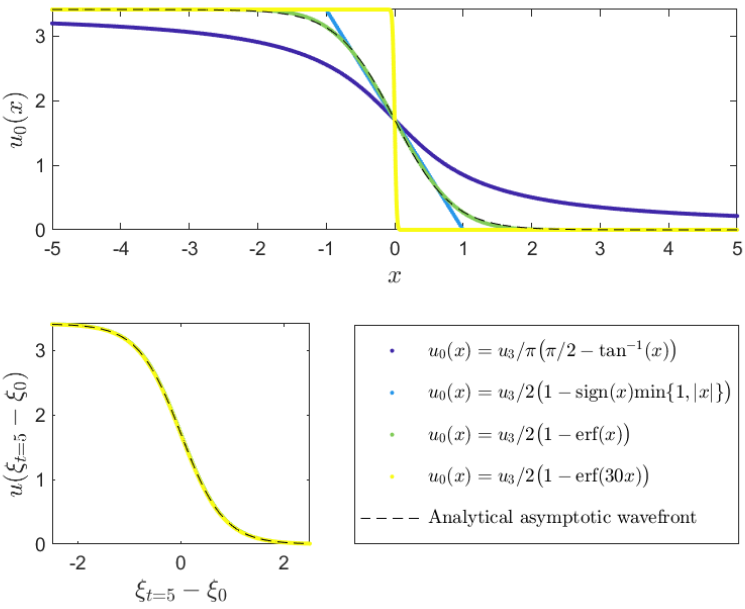

Figure 3: *Asymptotic shape of the traveling front is independent of initial condition.* The TDGLE was solved in the interval $x \in [-100, 100]$ for the case of $u_3 = 2 + \sqrt{2}$, with 4 different initial conditions (see legend). **Top,** the initial conditions $u_0(x)$. **Bottom,** the solution at $t = 5$ for each initial condition, as a function of the space-time coordinate $\xi = x - ct$, shifted by ξ_0 (different for each of the initial conditions used). c and ξ_0 are the fitting coefficients from the linear fit to $x_{front}(t)$ (see caption of Fig. 2 for a more detailed account). The analytical shape of the traveling front at long times (Eq. 5) is imposed as a dashed line for comparison in both panels.

Looking at the dynamics of the solution at short times, a clear convergence of shape and velocity is evident, and both processes seem to occur simultaneously. A brief look at the solution as a function of the traveling coordinate ξ shows that there exist a point on the solution that has a fixed "position" ξ^* and a fixed value u^*, such that $u\big(\xi^*(x(t) - ct)\big) = u^*$ at all t, thus it is traveling with exactly the velocity c of the asymptotic front. It might be argued that it would be better to define $x_{front}(t)$ as the point at which $u(x_{front}, t) = u^*$, so that convergence issues are avoided when looking to compute this velocity. Interestingly however, it seems that ξ^* has no clear relation to ξ_0, nor u^* to $f(u)$, and that both ξ^* and u^* depend on the specific structure of the initial condition introduced to the equation, making this advantage unreliable in the lack of a more thorough analysis.

Luckily, convergence times are of order $\mathcal{O}(1)$, so that even $t_{final} = 5$ is sufficient with most conventional initial conditions one can think of. The convergence of the shape of the traveling front to its asymptotic form is robust and is of course independent of the initial condition. A convergence of shape at $t = 5$ in a few representative cases is shown in Fig. 3, demonstrating the above statement to

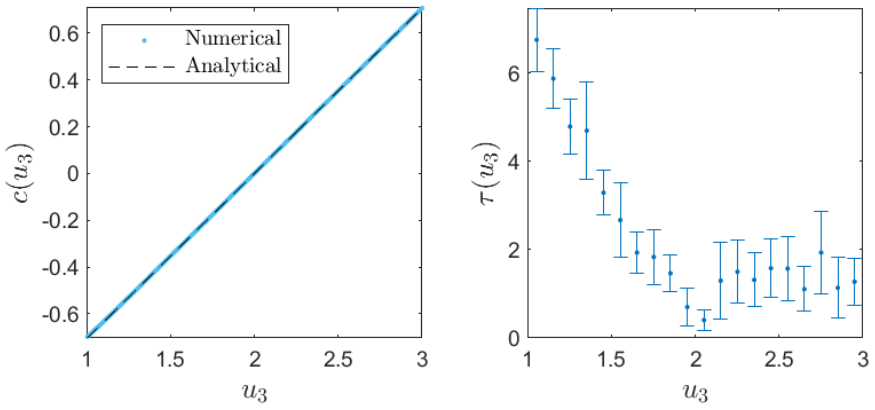

Figure 4: *Area rule (i.e. Maxwell's rule) and convergence times.* **Left,** the velocity c of the traveling front as a function of the reaction parameter u_3, as computed from linear fitting the wavefront $x_{front}(t)$ (in blue - see caption of Fig. 2 for a more detailed account). The TDGLE was solved in the interval $x \in [-100, 100]$ with an initial condition $u_0(x) = \frac{u_3}{2}\big(1 - \mathrm{erf}(x)\big)$. Note that $c(u_3 = 2) = 0$, as the two areas under the curve of the reaction function $f(u)$ are equal at this value (see Fig. 1 and *"area rule"* in the text). The analytical expression for $c(u_3)$ (see Eq. 6) is imposed on the data as a dash line for comparison. **Right,** convergence time, defined as the first time at which $\xi - \xi_0$ is of the same order of magnitude as after convergence, as a function of the reaction parameter u_3. Due to the deterministic nature of the solver, convergence time was computed at many points from which a smaller amount of points were acquired through computation of Gaussian-ly weighted (local) averages and standard deviations of the raw data (20 raw values per point).

a high level of accuracy. Note that convergence time becomes larger as u_3 gets closer and closer to 1, so that the statement does not necessarily hold, as explained in the following paragraphs.

Next, the process of finding the velocity c of the asymptotic traveling front solution was repeated for a range of u_3 values, using an initial condition $u_0(x) = \frac{u_3}{2}\big(1 - \mathrm{erf}(x)\big)$, which is close in shape to the asymptotic form in Eq. 5 (see green curve in top panel of Fig. 3), in order to shorten convergence times. Expecting a simple linear relation, and in light of the "area rule", a symmetric range around the point $u_3 = 2$ of equal areas (under the curve of $f(u)$) was chosen for evaluation of c, starting just above the qualitative dynamical change at $u_3 = 1$, for which $f(u)$ has only two fixed points and is not bistable in nature, up to $u_3 = 3$. From Fig. 4, it is clear that the numerical results are precisely captured by the theoretical relation in Eq. 6, numerically validating the "area rule" for the chosen reaction function $f(u)$.

Using the same starting point in time for fitting the velocity as in previous shown cases, produced results that deviate from the theoretical predictions more and more as u_3 gets closer to 1. This is due to the fact that the time for the dynamics to converge increases as $f(u)$ gets closer to the point where it is no longer bistable, which affects the dynamics significantly. To overcome this discrepancy between prediction and results, the fits for the velocity for $u_3 < 1.5$ were computed starting from $t = 10$.

In order to characterize this dependence, the time at which $\xi - \xi_0$ is of the same order of magnitude as its value after convergence, i.e. τ, was computed using the same data as in the process of finding the relation $c(u_3)$. Values of τ that are computed this way show the main expected trend, however they introduce a large scatter. To overcome this scatter, local averages and their corresponding standard deviation, both weighted with a Gaussian function, were computed and are shown in Fig. 4. At the range $1 < u_3 < 2$, convergence times decline steeply as u_3 increases, until reaching a deep around $u_3 \sim 2$, where the velocity of the traveling front is very small. Interestingly, above the point of equal areas, at the range $u_3 > 2$, convergence time seems to be largely unaffected by changes in u_3. It looks as though the dependence of τ on u_3 is by enlarge unaffected by the magnitude of c (excluding the deep for $c \sim 0$), and is mostly determined by the proximity to $u_3 = 1$, where dynamics change qualitatively.

3 Conclusion

In this work, we checked the validity of the assumption of the existence of traveling front solutions to the TDGLE. This was based on using the bistability property of the reaction function of the TDGLE, and generating a competition between its two stable phases, which manifests itself as a traveling front that forms after a short transient, leading to the dominion of the globally stable phase, which is chosen by the shape of the reaction function, as $t \to \infty$.

In addition, the dynamics and basic features of TDGLE were characterized in order to verify the theoretical predictions regarding the asymptotic shape and velocity of the traveling front solutions. It was shown that the asymptotics of the dynamics are robust, and are independent of initial conditions, and that the theoretical predictions accurately capture the numerical results in both aspects, demonstrating the "area rule" for the TDGLE.

We identified a dependence of convergence times on the reaction parameter u_3, and an attempt to characterize this dependence was carried out, showing a clear general trend, and giving some insight regarding the role of bistability in determining the dynamics of the TDGLE.